Theoretical study of an actively mode-locked fiber laser stabilized by an intracavity Fabry–Perot etalon: linear regime

Yurij Parkhomenko,[1] Moshe Horowitz,[1,*] Curtis R. Menyuk,[2] and Thomas F. Carruthers[3,4]

[1]*Department of Electrical Engineering, Technion–Israel Institute of Technology, Haifa 32000, Israel*
[2]*Department of Computer Science and Electrical Engineering, University of Maryland Baltimore County, 1000 Hilltop Circle, Baltimore, Maryland 21250, USA*
[3]*Optical Sciences Division, Naval Research Laboratory, Washington, D.C. 20375, USA*
[4]*Present address, Physics Division, National Science Foundation, Arlington, Virginia 22230, USA.*
[*]*Corresponding author: horowitz@ee.technion.ac.il*

Received December 1, 2006; accepted January 9, 2007;
posted January 31, 2007 (Doc. ID 77679); published July 19, 2007

We study theoretically the effect of an intracavity etalon on actively mode-locked fiber lasers by solving the master equation for the laser when nonlinearity in the laser is negligible. The first-order dispersion of the material inside the etalon can increase the pulse duration by a factor of 10. The minimum pulse duration is obtained when the relative frequency offset between the free spectral range of the etalon and the modulation frequency of the active mode locking is of the order of 10^{-2}. The group-velocity dispersion of the material inside the etalon as well as the finesse of the etalon affect the total cavity dispersion. The etalon helps to suppress both a simultaneous lasing in several supermodes and lasing in higher-order pulse modes of the master equation. The etalon also helps lock the central wavelength of the laser to the etalon comb. © 2007 Optical Society of America

OCIS codes: 140.4050, 140.3510, 060.2310, 050.2230, 140.3410.

1. INTRODUCTION

Actively mode-locked fiber lasers are important pulsed sources due to their ability to generate a train of short pulses with a high repetition rate and a very low jitter [1–3]. To improve the performance of fiber lasers, one must reduce the noise, stabilize their operation, and eliminate pulse dropout. One of the methods to stabilize actively mode-locked fiber lasers is to use an intracavity Fabry–Perot etalon [4–7].

The effect of an intracavity etalon on the pulses of an actively mode-locked fiber laser has been studied experimentally [4–7]. A theoretical study of a laser with an intracavity etalon is given in Ref. [7]. However, in this work, the effect of the cavity dispersion and the dispersion of the material inside the etalon was not taken into account. The work was also based on assuming a Gaussian pulse profile, rather than obtaining all the possible pulse modes by solving a master equation. In Ref. [8], the effect of an intracavity etalon on a pulse's duration was theoretically studied. However, the assumption in this work was that the bandwidth of a single etalon mode is large compared with both the axial mode spacing of the laser and the pulse bandwidth. In a fiber laser that generates short pulses of the order of 10 ps with a repetition rate of a few gigahertz, the mode spacing of the etalon is approximately equal to mode spacing between the laser modes [4–7] as studied in this paper. We also show that the material dispersion inside the etalon that was neglected plays an important role in determining the pulse duration in fiber lasers.

In the present paper, we theoretically study a laser that contains an intracavity etalon by deriving and solving an appropriate master equation that includes terms that are due to the intracavity etalon. The solution of the master equation gives the dependence of the pulse duration on the parameters of the etalon assuming that nonlinearity is negligible. In particular, we show that the first-order dispersion caused by the etalon material significantly increases the pulse duration. We show that the minimum pulse duration is obtained when there is a small detuning of the order of 1% between the free spectral range of the etalon and the frequency difference between the laser modes. We also show that the group-velocity dispersion of the material inside the etalon and the etalon finesse should be taken into account when calculating the cavity dispersion. Therefore, the insertion of the etalon may increase or decrease the pulse duration, depending on the sign of the second-order etalon dispersion. The etalon helps to suppress a simultaneous lasing in several supermodes as well as suppressing lasing in higher-order pulse modes of the master equation. The etalon also helps to lock the center frequency of the laser. Therefore, the use of an intracavity etalon eliminates the need to control the length of the laser cavity, which is required when the laser is locked to an external etalon [9]. The filtering from the intracavity etalon can be more than three times stronger than the filtering from an external etalon with the same finesse. By appropriately choosing the cavity dispersion, the etalon finesse, and the dispersion of the material inside the etalon, the minimum pulse duration can be

Report Documentation Page

Form Approved
OMB No. 0704-0188

1. REPORT DATE	2. REPORT TYPE	3. DATES COVERED
JAN 2007		**00-00-2007 to 00-00-2007**

4. TITLE AND SUBTITLE	5a. CONTRACT NUMBER
Theoretical study of an actively mode-locked fiber laser stabilized by an intracavity Fabry-Perot etalon: linear regime	5b. GRANT NUMBER
	5c. PROGRAM ELEMENT NUMBER
6. AUTHOR(S)	5d. PROJECT NUMBER
	5e. TASK NUMBER
	5f. WORK UNIT NUMBER
7. PERFORMING ORGANIZATION NAME(S) AND ADDRESS(ES) **University of Maryland Baltimore County,Department of Computer Science and Electrical Engineering,1000 Hilltop Circle,Baltimore ,MD,21250**	8. PERFORMING ORGANIZATION REPORT NUMBER
9. SPONSORING/MONITORING AGENCY NAME(S) AND ADDRESS(ES)	10. SPONSOR/MONITOR'S ACRONYM(S)
	11. SPONSOR/MONITOR'S REPORT NUMBER(S)

12. DISTRIBUTION/AVAILABILITY STATEMENT
Approved for public release; distribution unlimited

13. SUPPLEMENTARY NOTES

14. ABSTRACT

15. SUBJECT TERMS

16. SECURITY CLASSIFICATION OF:			17. LIMITATION OF ABSTRACT	18. NUMBER OF PAGES	19a. NAME OF RESPONSIBLE PERSON
a. REPORT **unclassified**	b. ABSTRACT **unclassified**	c. THIS PAGE **unclassified**	**Same as Report (SAR)**	**10**	

equal to the Kuizenga–Siegman limit of a laser without dispersion [8].

The paper is organized as follows. In Section 2, we derive the master equation for a laser with an intracavity etalon. The master equation is solved in Section 3. The effect of the etalon parameters on the pulse duration and on the suppression of higher-order lasing modes is analyzed using numerical examples in Section 4. In Section 5, we show that the etalon helps to suppress simultaneous lasing in several supermodes. We determine the optimal etalon finesse and the optimal detuning between the free spectral range of the etalon and the spacing between laser modes that are required in order to obtain a large suppression of supermode competition without a significant increase in the pulse duration.

2. MATHEMATICAL MODEL FOR THE LASER

Our mathematical model of the laser is similar to the master-equation model developed by Haus [10]. A schematic of an actively mode-locked ring fiber laser is shown in Fig. 1. The laser uses an erbium-doped fiber amplifier with a broad bandwidth and a slow relaxation time, of the order of hundreds of microseconds. The laser cavity also includes an optical filter, a sinusoidally varying amplitude modulator at a frequency Ω_M, an isolator for obtaining a unidirectional oscillation, a fiber with a length L, and a Fabry–Perot etalon with a free spectral range Ω_e and a finesse F. To obtain the optimal performance of the laser, we assume that the modulation frequency, $\Omega_M/2\pi$, is equal to the inverse of the round-trip time of a pulse inside the cavity multiplied by an integer number. This condition can be met in fiber lasers by using a tunable delay line connected to an electro-optic feedback circuit [1]. We denote the gain and the FWHM of the gain profile by g and $2\Omega_g$, and we denote the loss and the FWHM of the optical filter by K and $2\Omega_K$, respectively. The central frequency of the amplifier is denoted by ω_g. We also assume that the central frequency of the optical filter is equal to the central frequency of the amplifier, as is required to obtain short pulses.

A. Spectral Transfer Function of the Etalon

The spectral transfer function of an etalon built up from two equal mirrors, with an intensity reflection coefficient R, is a periodic function of the frequency [11,12]

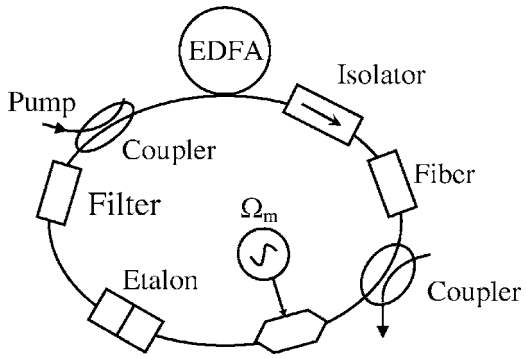

Fig. 1. Schematic of the laser cavity that is analyzed in this paper. EDFA, an erbium-doped fiber amplifier.

$$T_F(\omega_{\text{tot}}) = \frac{(1-R)\exp(i\varphi/2)}{1-R\exp(i\varphi)}, \tag{1}$$

where ω_{tot} is the angular frequency, $\varphi = 2\omega_{\text{tot}} n(\omega_{\text{tot}}) l/c$ is the phase accumulated in one round trip, n is the refractive index of the material inside the etalon, c is the light velocity, and l is the etalon length. The exponent in the numerator of Eq. (1) is equivalent to propagation through a dielectric slab with a length l and a refractive index n, and it can therefore be omitted from the transfer function and put back elsewhere. In this case, the transfer function of the etalon becomes $T_E(\omega_{\text{tot}}) = T_F(\omega_{\text{tot}})\exp(-i\varphi/2)$. The optical spectrum of laser pulses is built from modes at discrete frequencies,

$$\omega_{\text{tot}} = \omega_0 + \delta\omega + N\Omega_e + N\Delta\Omega, \tag{2}$$

where $\Delta\Omega = \Omega_M - \Omega_e$, $N = 0, \pm 1, \pm 2, \ldots$ is an integer, $\Omega_e = \pi c/ln(\omega_0)$ is the free spectral range of the etalon at a frequency ω_0, and ω_0 is the resonance frequency of the etalon that is closest to the central frequency of the laser amplifier, ω_g. The FWHM of an etalon mode is equal to Ω_e/F where $F = \pi\sqrt{R}/(1-R)$ is the etalon finesse [12]. The frequency offset $\delta\omega$ is the frequency detuning of the laser frequency comb relative to the etalon comb at $N = 0$. Figure 2 illustrates the notation used in Eq. (2).

The width of the etalon modes is significantly greater than the width of the laser modes. Experimental results indicate that the width of the laser modes is of the order of a few kilohertz [13,14]. On the other hand, the width of

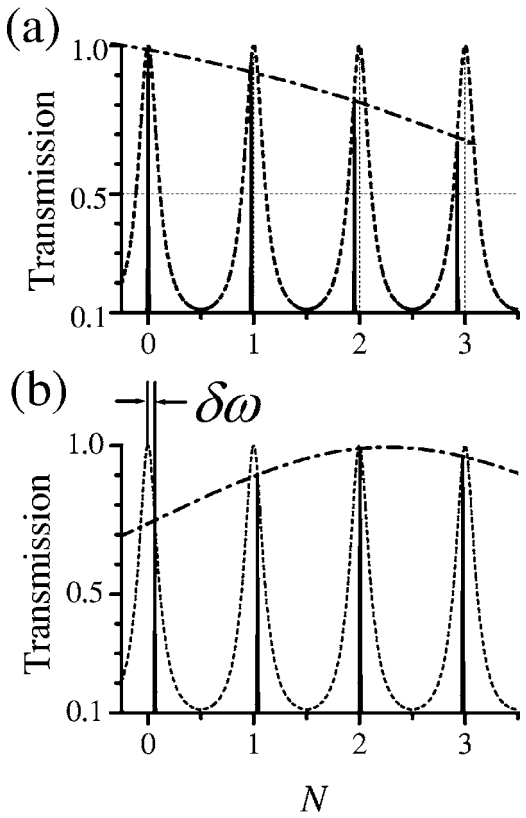

Fig. 2. Schematic of the etalon modes (dotted curve) and the modes of the laser (solid line) when (a) $\delta\omega = 0$, (b) $\delta\omega \neq 0$. The parameter N is the mode number. The dashed–dotted curve represents the etalon filtering.

the etalon modes is of the order of tens of megahertz. Therefore, we will calculate the transfer function of the etalon only at the frequencies of the laser modes.

To obtain narrow pulses and avoid a significant increase in the cavity loss, the frequency offsets $\delta\omega$ and $\Delta\Omega$ should both be small compared with the width of the etalon modes, so that $\delta\omega, \Delta\Omega < \Omega_e/F$, as shown in Fig. 2. In actively mode-locked lasers, the pulse bandwidth is always smaller than the carrier frequency, and hence $|N_{\max}|\Omega_M \ll \omega_0$. In the numerical example given in Section 4, we use $\lambda_0 = 1.55\ \mu$m, $\omega_0 = 1.2\times10^{15}$ rad/s, $\Omega_M/2\pi = 10$ GHz, an etalon finesse $F = 100$, from which we obtain $|N_{\max}| \approx 3.2$, $2|N_{\max}|\Omega_e \approx 4\times10^{11}$ rad/s, $\Delta\Omega/\Omega_e \approx 0.01$, and $\delta\omega/\Omega_e \approx 10^{-4}$. These values correspond to experiments [4–7]. Hence, we may use the ordering,

$$\omega_{\text{tot}} = \epsilon^{-1}\omega_0 + N\Omega_e + \epsilon(\delta\omega + N\Delta\Omega), \tag{3}$$

where ϵ is an ordering parameter, which we will eventually set equal to 1. As usual in this sort of expansion, the ordering parameter is used to keep track of the relative magnitude of components. Terms proportional to higher powers of ϵ are smaller than those at lower power. We will take into account in our calculations the effect of the material dispersion inside the etalon up to second order in the frequency difference, $\omega_{\text{tot}} - \omega_0$. We choose to use a single ordering parameter for the changes in both the refractive index and the frequency. Since $|N_{\max}|\Omega_M \ll \omega_0$, we obtain

$$n(\omega) = n_0 + \epsilon^2\gamma_1[N\Omega_e + \epsilon(\delta\omega + N\Delta\Omega)] + \epsilon^3\gamma_2[N\Omega_e + \epsilon(\delta\omega + N\Delta\Omega)]^2, \tag{4}$$

where $n(\omega)$ is the refractive index of the material inside the etalon, $\gamma_1 = dn/d\omega_{\text{tot}}|_{\omega_0}$, $\gamma_2 = (1/2)d^2n/d\omega_{\text{tot}}^2|_{\omega_0}$. For bulk fused silica at $\lambda = 1.55\ \mu$m, we obtain $n_0 = 1.44$, $\gamma_1\omega_0 = 1.86\times10^{-2}$, $\gamma_1\Omega_e = 9.6\times10^{-7}$, $\gamma_2\omega_0\Omega_e = -1.22\times10^{-6}$, $\gamma_2\Omega_e^2 = -6.3\times10^{-11}$, and $|(\gamma_1/n_0)/(\gamma_2/\gamma_1)| = 0.01$.

The accumulated phase in the etalon φ, given in Eq. (1), can be decomposed into successive orders,

$$\varphi = \epsilon^{-1}\varphi_{-1} + \varphi_0 + \epsilon\varphi_1 + \epsilon^2\varphi_2, \tag{5}$$

where

$$\varphi_{-1} = \frac{2l}{c}n_0\omega_0 = 2\pi m, \tag{6a}$$

$$\varphi_0 = \frac{2l}{c}n_0 N\Omega_e = 2\pi N, \tag{6b}$$

$$\varphi_1 = \frac{2l}{c}n_0(\delta\omega + Nh), \tag{6c}$$

$$\varphi_2 = \frac{2l}{c}[\gamma_1\omega_0(\delta\omega + N\Delta\Omega) + (\gamma_1 + \gamma_2\omega_0)\times(N\Omega_e)^2], \tag{6d}$$

$$h = \Delta\Omega + \Omega_e\gamma_1\omega_0/n_0, \tag{6e}$$

and m is an integer. The parameter h denotes the difference between the free spectral range of the etalon and the frequency difference between the laser modes. The second term in the parameter h describes the effect of the dispersion of the material inside the etalon on the free spectral range of the etalon. The result obtained for φ_{-1} and φ_0 gives the etalon resonance condition.

By substituting the Taylor expansion given in Eq. (5) into Eq. (1), we obtain

$$T_E(\varphi) = 1 + \left.\frac{\partial P}{\partial\varphi}\right|_{\varphi=0}(\epsilon\varphi_1 + \epsilon^2\varphi_2) + \frac{1}{2}\left.\frac{\partial^2 P}{\partial\varphi^2}\right|_{\varphi=0}(\epsilon\varphi_1 + \epsilon^2\varphi_2)^2$$

$$\cong 1 + i\frac{\sqrt{JR}}{2}(\epsilon\varphi_1 + \epsilon^2\varphi_2) - \epsilon^2 J(1+R)\frac{\varphi_1^2}{8} + O(\epsilon^3), \tag{7}$$

where J is the finesse coefficient, given by $J = 4R/(1-R)^2$. By substituting Eq. (6) into Eq. (7), we obtain

$$T_E(\omega_{\text{tot}}) = \bar{P}_0 + \bar{P}_1\epsilon + \bar{P}_2\epsilon^2, \tag{8}$$

where

$$\bar{P}_0 = 1,$$

$$\bar{P}_1 = \left[iC_2\left(\frac{2ln_0}{c}\right)\delta\omega\right] + \left[iC_2\left(\frac{2ln_0}{c}\right)h\right]N,$$

$$\bar{P}_2 = \left[iC_2\left(\frac{2ln_0}{c}\right)(\gamma_1/n_0)\omega_0\Delta\omega + C_1\left(\frac{2ln_0}{c}\right)^2(\delta\omega)^2\right] + \left[iC_2\left(\frac{2ln_0}{c}\right)(\gamma_1/n_0)\omega_0\delta\Omega + C_1\left(\frac{2ln_0}{c}\right)^2 2h\,\delta\omega\right]N + \left[iC_2\left(\frac{2ln_0}{c}\right)[(\gamma_1 + \omega_0\gamma_2)/n_0]\Omega_e^2 + C_1\left(\frac{2ln_0}{c}\right)^2 h^2\right]N^2, \tag{9}$$

with $C_1 = -J(1+R)/8$ and $C_2 = \sqrt{JR}/2$.

Equation (8) can be ordered as

$$T_E(N) = \tilde{P}_0 + \tilde{P}_1 N + \tilde{P}_2 N^2, \tag{10}$$

where

$$\tilde{P}_0 = 1 - \frac{J(1+R)}{8}(2ln_0/c)^2\delta\omega^2 + i\frac{\sqrt{JR}}{2}\frac{2l}{c}(\omega_0\gamma_1\delta\omega + n_0\delta\omega),$$

$$\tilde{P}_1 = -\frac{J(1+R)}{8}(2ln_0/c)^2 2h\,\delta\omega + i\frac{\sqrt{JR}}{2}\frac{2l}{c}(hn_0 + \omega_0\gamma_1\Delta\Omega),$$

$$\tilde{P}_2 = -\frac{J(1+R)}{8}(2ln_0/c)^2h^2 + i\frac{\sqrt{JR}}{2}\frac{2l}{c}(\gamma_1 + \omega_0\gamma_2)\Omega_e^2. \tag{11}$$

From here on, we set $\epsilon = 1$.

B. Master Equation for Pulse Spectrum

The field in the laser cavity is built from a train of pulses,

$$E(T,t) = \sum_m a_m(T, t - mT_M), \tag{12}$$

where T_M is repetition rate of the pulses, $T_M = 2\pi/\Omega_M$, T is a slow time variable of the order of the cavity round-trip time, t is a fast time variable of the order of the pulse duration, and $a_m(T,t)$ is the field envelope of the mth pulse defined around a reference frequency that is equal to the frequency of the laser mode at $\omega_0 + \delta\omega$. Without the etalon, the master equation is developed for a pulse with a carrier frequency that is equal to the central frequency of the amplifier gain, ω_g. However, since the bandwidth of the filter and the amplifier are significantly broader than the free spectral range of the etalon and the modulation frequency of the laser, the effect of the frequency difference $\omega_g - (\omega_0 + \delta\omega)$ on the parameters of the master equation can be neglected. In the example given in Section 4, the modulation frequency and the free spectral range of the etalon are approximately equal to $2\pi \times 10^{10}$ rad/s, while the bandwidths of the amplifier gain and the filter are equal to $\Omega_g = 5.5 \times 10^{12}$ and $\Omega_K = 3.9 \times 10^{12}$ rad/s, respectively. Therefore, the change in the filter loss due to the frequency difference $\omega_g - (\omega_0 + \delta\omega)$ is less than 6×10^{-6}.

We neglect in our analysis the nonlinear Kerr effect. This neglect enables us to obtain a simple solution and it is justified since the pulses that were experimentally obtained in fiber lasers with an intracavity etalon had a broad duration of ~10–100 ps [4–7]. The master equation for the mth pulse of the pulse train is given by

$$T_R \frac{\partial a_m(T,t)}{\partial T} = (g - \delta) a_m(T,t) + \left(iD + \frac{g}{\Omega_g^2} + \frac{K}{\Omega_K^2} \right) \frac{\partial^2 a_m(T,t)}{\partial t^2} - M[1 - \cos(\Omega_M t)] a_m(T,t) + w_m(T,t), \tag{13}$$

where δ is the laser loss per a single round trip, T_R is the round-trip time, D is the overall cavity group-velocity dispersion coefficient ($D > 0$ represents the anomalous dispersion region), M is the modulation depth, and Ω_g, Ω_K, g, and K are the FWHM and the gain and loss of the amplifier and the filter, respectively. We are using the negative carrier frequency convention. The filter loss that is frequency independent is included in the constant loss δ. The pulse duration is significantly shorter than the period of the mode locking, $T_M = 2\pi/\Omega_M$, and therefore the transmission of the modulator can be approximated by $M[1 - \cos(\Omega_M t)] \approx M(\Omega_M t)^2/2$. The function $w_m(T,t)$ represents the response of the etalon. When the dispersion of the material inside the etalon can be neglected the change in the mth pulse due to the etalon is given by

$$w_m(T,t) = (1 - R) \sum_{j=0}^{\infty} R^j a_{m-j}[T, t - j(T_M - T_e)] - a_m[T,t], \tag{14}$$

where $T_e = 2l/(cn_0)$ is the round-trip time of a pulse in the etalon. Equation (14) shows that in the time domain, the etalon couples neighboring pulses. The number of pulses that are coupled is approximately equal to the finesse of the etalon.

The effect of the etalon on the laser may be analyzed in the frequency domain, allowing us to include the effect of dispersion inside the etalon. Assuming that all the laser pulses are the same, i.e., $a_m(T,t) = a(T,t)$, we can calculate the transfer function of the etalon in the frequency domain for one of the cavity pulses. To use Eqs. (1) and (10) for calculating the etalon transmission, the lifetime of a single pulse in the etalon must be smaller than the effective round-trip time of the pulse in the laser cavity, which will be true as long as the finesse of the intracavity etalon is smaller than the number of pulses that simultaneously propagate in the cavity. For example, in a laser with a cavity length of ~100 m and with a repetition frequency of 10 GHz, approximately 5000 pulses simultaneously propagate inside the cavity, while the typical finesse of an intracavity etalon is only of the order of a few hundred. Since the lifetime of a pulse in the etalon is approximately equal to FT_e, we may neglect coupling between pulses that propagate a different number of round trips in the cavity. On the other hand, since the etalon causes coupling among a large number of pulses, the pulses inside the cavity will be mutually coherent. Hence, we obtain

$$w(T,t) = (1 - R) \sum_{j=0}^{\infty} R^j a[T, t - j(T_M - T_e)] - a[T,t]. \tag{15}$$

The first term in the right-hand side of Eq. (15) is equal to the transfer function of etalon in the time domain when dispersion is neglected. The effect of dispersion on the etalon can be added in the frequency domain after making a Fourier transformation of Eq. (15). The detuning between the etalon and the laser cavities $T_M - T_e$ is converted in the frequency domain to a linear phase shift that accumulates in one round trip. The effect of the first- and second-order dispersion at $\omega_0 + \delta\omega$ can then be added. The result reproduces Eq. (1), as expected. Using the approximate transmission of the etalon for the laser modes, we substitute $N = [\omega_{\text{tot}} - (\omega_0 + \delta\omega)]/\Omega_M \equiv \omega/\Omega_M$ into Eq. (10) and obtain

$$T_E(\omega) = P_0 + P_1\omega + P_2\omega^2,$$

$$w(T,\omega) = \tilde{a}(T,\omega)[T_E(\omega) - 1], \tag{16}$$

where

$$P_i = \frac{\tilde{P}_i}{(\Omega_M)^i} \quad (i = 0, \ldots, 2). \tag{17}$$

We note that ω is the frequency difference, calculated with respect to a reference frequency that is equal to the laser mode at $\omega_0 + \delta\omega$, and the pulse spectrum, $\tilde{a}(T,\omega)$, is the Fourier transform of the pulse profile $a(T,t)$

$$\tilde{a}(T,\omega) = \int_{-\infty}^{\infty} dt \exp(i\omega t) a(T,t). \tag{18}$$

The master equation, written in the frequency domain, becomes

$$T_R\frac{\partial\tilde{a}(T,\omega)}{\partial T}=\frac{M}{2}\Omega_M^2\frac{\partial^2\tilde{a}(T,\omega)}{\partial\omega^2}-\left(iD+\frac{g}{\Omega_g^2}+\frac{K}{\Omega_K^2}-P_2\right)\times\omega^2\tilde{a}(T,\omega)+[g-\delta+\mathrm{Re}(P_0-1)]\tilde{a}(T,\omega)+\omega\,\mathrm{Re}(P_1)\tilde{a}(T,\omega). \quad (19)$$

The parameters of the etalon, P_i, $i=0,1,2$, are defined in Eqs. (11) and (17). The term $\mathrm{Im}(P_0)$ gives the change in the accumulated phase of the pulses, and, therefore, it only slightly changes the effective cavity length. The terms proportional to $\mathrm{Re}(P_0)$ and $\mathrm{Re}(P_1)$ describe the constant and the linear frequency-dependent loss due to the etalon. The real and the imaginary part of the term proportional to P_2 describe the second-order loss and the dispersion caused by the etalon, respectively. We note that the time T_R is determined by the group velocity V_g of all the cavity elements including the etalon. Hence, the contribution from $\mathrm{Im}(P_1)$ is included in T_R and does not appear separately.

3. SOLUTION OF THE MASTER EQUATION

In a practical fiber laser, the frequency difference between the cavity modes is significantly smaller than the bandwidth of the etalon modes. For example, in a ring laser with a length of 100 m, the frequency difference between two neighboring modes is 2 MHz. Assuming an etalon with a free spectral range of 10 GHz and a finesse of $F=100$, there should be ~50 laser modes inside a single etalon mode. Therefore, in such a laser, we may set $\delta\omega\approx 0$ and hence $\mathrm{Re}(P_1)\approx 0$. A solution of Eq. (19) when $\delta\omega\neq 0$ will be given in Section 5. In the case when $\mathrm{Re}(P_1)\approx 0$, the solution of Eq. (19) can be represented as a series of Hermite–Gaussian modes,

$$\tilde{a}(T,\omega)=\sum_{m=0}^{\infty}c_m\exp\left(-\frac{\omega^2}{2}\tau_m^2\right)H_m(\omega\tau_m)\exp\left(\frac{T}{T_R}\Lambda_m\right), \quad (20)$$

where $H_m(x)$ are Hermite polynomials of the order of m, c_m is the mode amplitude, and the parameters τ_m and Λ_m are obtained from the relations

$$\tau_m^4=W/s, \quad (21a)$$

$$\Lambda_m=g_m-\delta-(2m+1)\sqrt{Ws}, \quad (21b)$$

where

$$s=\frac{M}{2}\Omega_M^2,\quad W=\frac{g_m}{\Omega_g^2}+\frac{K}{\Omega_K^2}+iD-P_2. \quad (22)$$

The inverse Fourier transform of the pulse spectrum is equal to

$$a(T,t)=\sum_{m=0}^{\infty}c_m\exp\left(-\frac{t^2}{2\tau_m^2}\right)H_m(t/\tau_m)\exp\left(\frac{T}{T_R}\Lambda_m\right). \quad (23)$$

Above the laser threshold, the net gain of the mth mode, $\mathrm{Re}(\Lambda_m)$, should be equal to zero. If the laser amplifier is homogeneously broadened, only the mode with the lowest net gain will be generated. In actively mode-locked fiber lasers, based on an erbium-doped fiber amplifier, the bandwidth of the amplifier is significantly broader than the bandwidth of the pulses. Therefore, the amplifier gain in our laser is mainly determined by the constant loss δ and by the etalon, as we show in the numerical example presented in Section 4. Hence, the parameter W does not strongly depend on the mode number. In this case, Eq. (21b) shows that the minimum threshold gain is obtained for the fundamental mode with $m=0$. The pulse parameter τ_0 obtained for this mode is given by

$$\tau_0=\left\{\frac{1}{2\Omega_g^2}+\left[\left(\frac{1}{2\Omega_g^2}\right)^2+\frac{\hat{P}-i\hat{D}}{s}\right]^{1/2}\right\}^{1/2}, \quad (24)$$

where

$$\hat{P}=\frac{\delta}{\Omega_g^2}+\frac{K}{\Omega_K^2}-\frac{J(1+R)}{8}(2ln_0/c)^2h^2\frac{1}{\Omega_M^2}, \quad (25)$$

$$\hat{D}=-D+\sqrt{JR}\frac{l}{c}(\gamma_1\Omega_e^2+\omega_0\gamma_2\Omega_e^2)\frac{1}{\Omega_M^2}-\frac{\mathrm{Im}(\Lambda_0)}{\Omega_g^2}. \quad (26)$$

Equation (25) implies that the etalon adds an effective filter to the laser cavity that is represented by the last term in Eq. (25). The etalon also adds an additional group-velocity dispersion to the laser cavity that is represented by the two final terms in Eq. (26). We note that the term $\gamma_1+\omega_0\gamma_2$ is equal to $(2/c)d^2\beta(\omega)/d\omega^2|_{\omega_0}$, where $\beta(\omega)$ is the propagation wavenumber in the etalon.

4. NUMERICAL EXAMPLE

In our numerical example, we will consider a laser with a configuration as described in Fig. 1 and with a modulation frequency $\Omega_M/2\pi=10$ GHz, a modulation index $M=0.2$, an accumulated group-velocity dispersion per round trip $D=0.13$ ps^2, and a constant loss $\delta=0.1$. The amplifier and the filter had a FWHM bandwidth of $2\Omega_g=2\times 5.5\times 10^{12}$ rad/s (20 nm) and $2\Omega_K=2\times 0.7\Omega_g$ (14 nm), respectively. We consider an etalon that is made of fused silica, so that the dispersion parameters are given by [12] $\gamma_1\omega_0=0.0186$, $\gamma_2\omega_0\Omega_M=-1.22\times 10^{-6}$. The length of the etalon is $l=1$ cm. We neglect the dispersion of the etalon mirrors.

We will present the chirped Gaussian pulses that are generated by the laser using the notation [15]

$$a(t)=a_0\exp\left[-\frac{(1+iC)}{2}\frac{t^2}{T_0^2}\right], \quad (27)$$

where $T_0=|\tau_0|^2/(\tau_R^2-\tau_I^2)^{1/2}$, $2T_0$ is the pulse duration at $1/e$ intensity points, $C=-2\tau_R\tau_I/(\tau_R^2-\tau_I^2)$ is the chirp parameter, $\tau_R=\mathrm{Re}(\tau_0)$, $\tau_I=\mathrm{Im}(\tau_0)$, and τ_0 is the pulse parameter obtained from Eq. (24). Figure 3(a) shows the dependence of the chirp parameter C and the normalized pulse duration $2T_0/2\tau_s$, where $2\tau_s$ is the Kuizenga–Siegman limit [8], on the detuning between the etalon and the laser modes, $\Delta\Omega$, for an etalon with a finesse $F=100$. The figure shows that a minimum pulse duration is obtained when the detuning $\Delta\Omega$ between the etalon and the laser modes

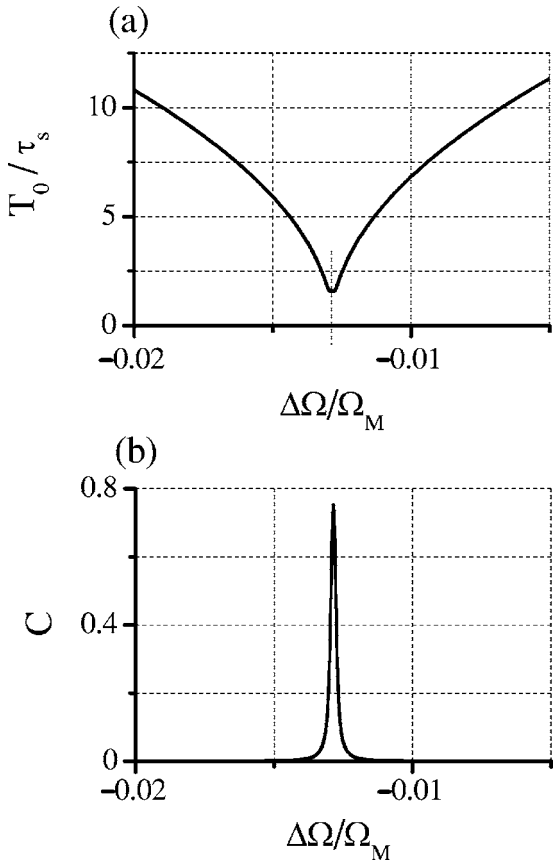

Fig. 3. (a) Pulse duration $2T_0$, normalized to the Kuizenga–Siegman limit $2\tau_s$ and (b) the chirp parameter C, as a function of the normalized frequency detuning between the etalon and the laser modes, $\Delta\Omega/\Omega_M$, for a laser with a modulation frequency $\Omega_M/2\pi=10$ GHz, a modulation depth $M=0.2$, a total cavity dispersion $D=0.13$ ps^2, a constant loss $\delta=0.1$, and an intracavity etalon with a finesse $F=100$ and with material dispersion coefficients $\gamma_1\omega_0=0.0186$, $\gamma_2\Omega_M\omega_0=-1.22\times10^{-6}$.

does not equal to zero. When substituting the parameters used to calculate Fig. 3 into Eqs. (25) and (26), we find that when $\Delta\Omega=0$, the first-order dispersion of the etalon material, γ_1, increases the parameters $\hat{P}$ and $\hat{D}$ by a factor of approximately 10^4 and 1.1, respectively, with respect to the case $\gamma_1=0$. The increase in the parameter $\hat{P}$ yields an increase in the pulse duration by a factor of approximately 10. It is possible to compensate for the increase in the parameter $\hat{P}$ due to the etalon material dispersion by adding a detuning $\Delta\Omega_{\min}$. Since in our example the gain and the filter dispersion make a small contribution to the parameter $\hat{P}$, the detuning parameter that gives a minimum pulse duration can be approximately calculated by requiring that $h=0$ and hence $\Delta\Omega_{\min}/\Omega_e\cong-\gamma_1\omega_0/n_0$.

It is necessary to detune the free spectral range of the etalon relative to the frequency spacing between the laser modes in order to obtain an optimal overlap between the laser modes and the etalon modes. The frequency spacing between the laser modes is almost independent of the frequency. On the other hand, the frequency spacing between the etalon modes depends on the frequency due to the dispersion of the material inside the etalon. The detuning between the etalon and the laser modes is needed to compensate for the first-order dispersion of the material inside the etalon.

The minimum pulse duration of $2T_0=9.4$ ps obtained in Fig. 3 is longer than the 6 ps Kuizenga–Siegman limit [8] because the dispersion parameter of the laser $\hat{D}$ does not equal zero. Equation (26) shows that the dispersion parameter $\hat{D}$ depends on the total cavity dispersion D as well as on the dispersion added by the etalon. The etalon dispersion is affected by the dispersion of the material inside the etalon and it increases as the finesse of the etalon increases. Therefore, in a laser with an etalon, the total dispersion is determined by the parameter $\hat{D}$ instead of total cavity dispersion D in a laser without an etalon. Figure 3(b) shows the chirp parameter C. The figure shows that a chirp is added when the pulse duration becomes minimum. The chirp decreases to zero as the detuning parameter deviates more from the point where a minimum pulse duration is obtained.

Figures 4 and 5 shows the dependence of the minimum pulse duration and the corresponding pulse chirp on the finesse of the etalon for two different signs of the total cavity dispersion D. In Fig. 4, the etalon adds a second-order dispersion with the same sign as the cavity dispersion (anomalous dispersion). In this case, the pulse duration increases as the etalon finesse increases as well as the pulse chirp. In the results shown in Fig. 5, the total cavity dispersion is normal and the etalon adds a second-order dispersion with an opposite sign to the cavity dispersion. In this case, when the etalon finesse increases,

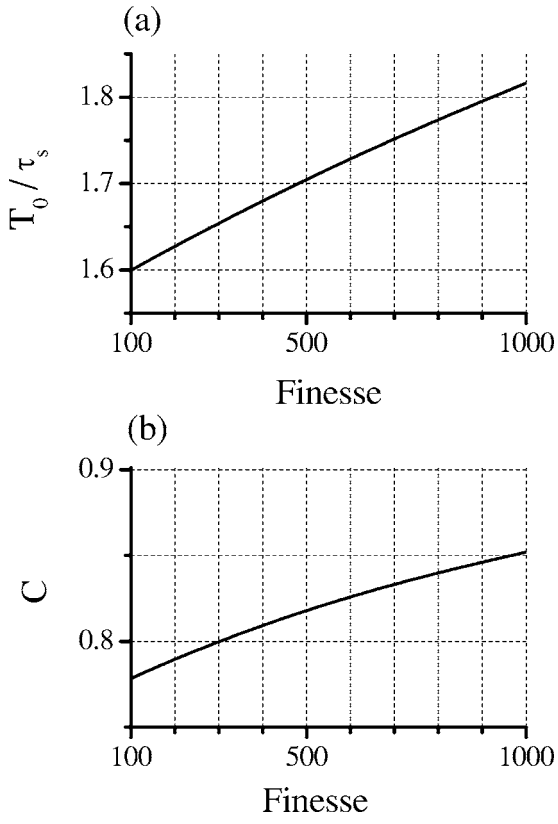

Fig. 4. Dependence of (a) the minimum pulse duration normalized to the Kuizenga–Siegman limit and (b) the chirp parameter on the etalon finesse calculated using the parameters in Fig. 3 and a normalized detuning, $\Delta\Omega/\Omega_M=-0.012858$.

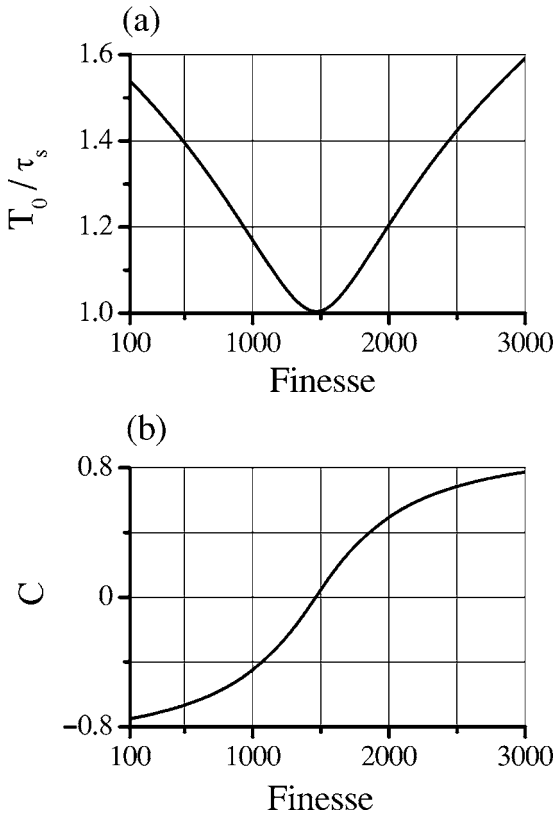

Fig. 5. Dependence of (a) the minimum pulse duration normalized to the Kuizenga–Siegman limit and (b) the chirp parameter on the etalon finesse calculated for a total cavity dispersion $D = -0.13$ ps^2 and a normalized detuning, $\Delta\Omega/\Omega_M = -0.012858$. The other laser parameters are as used in Fig. 3.

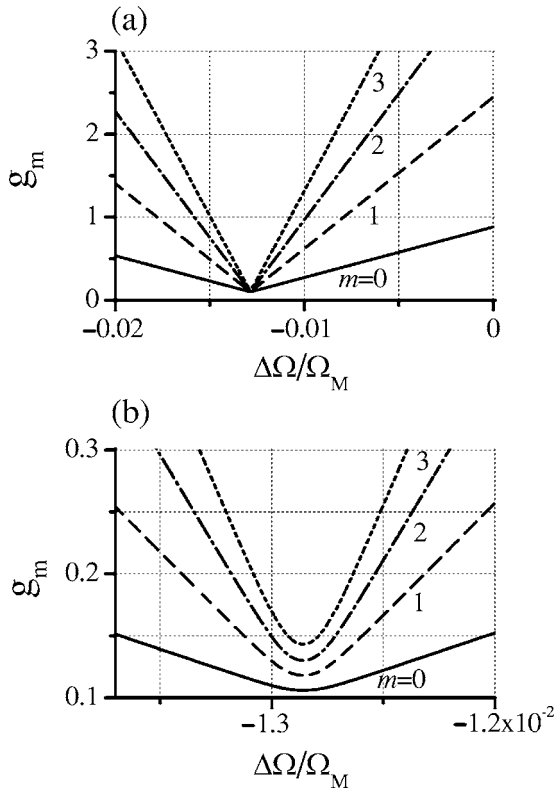

Fig. 6. (a) Dependence of threshold gain, g_m, for different pulse modes: $m = 0$ (solid line), 1 (dashed line), 2 (dashed-dotted line), 3 (dotted line). (b) A close-up view near the point where the minimum pulse duration is obtained. The parameters of the laser are the same as used in Fig. 3.

the pulse duration decreases until the pulse duration becomes equal to Kuizenga–Siegman limit of $2T_0 = 6$ ps for the laser. This limit is reached when the finesse is about $F = 1500$. At this point, the total cavity dispersion, $\hat{D}$, is approximately equal to zero. A further increase in the finesse increases the pulse duration since the total cavity dispersion begins to increase. Therefore, when the cavity dispersion, the etalon finesse, and the dispersion of the material inside the etalon are appropriately chosen, the insertion of the intracavity etalon will not increase the minimum pulse duration that can be generated by the laser.

Figure 6 shows dependence of the minimum gain $\mathrm{Re}(g_m)$ that is needed for different laser modes in a steady-state condition as a function of the detuning parameter, $\Delta\Omega$. The steady-state gain parameter g_m was calculated by solving the equation, obtained from Eq. (21),

$$g_m = \delta + (2m+1)\mathrm{Re}\left[\frac{M\Omega_M^2}{2}\left(\frac{g_m}{\Omega_g^2} + \frac{K}{\Omega_K^2} + iD - P_2\right)\right]^{1/2}. \tag{28}$$

Figure 6 shows that the minimum gain is obtained for the zero-order mode ($m = 0$). The minimum gain is obtained for the detuning frequency $\Delta\Omega = \Delta\Omega_{\min}$ that gives the minimum pulse duration. The difference between the gain of different modes increases as the absolute difference between the detuning frequencies $|\Delta\Omega - \Delta\Omega_{\min}|$, increases. Therefore, the laser becomes more stable as the pulse duration increases. In the general case, it is not straightforward to solve Eq. (28) since the gain g_m appears on both sides of the equation. However, in a fiber laser, the constant loss δ that does not depend on the pulse, can be as high as 10 dB [3]. Moreover, the bandwidths of the filter and the amplifier are significantly broader than the bandwidth of the pulse. Therefore, the main contribution to the gain is caused by the etalon, represented by the term P_2 in Eq. (28) and by the constant loss δ. Hence, Eq. (28) indicates that the minimum gain increases as the mode number m increases, due to the etalon filtering effect. As the mode number increases, the bandwidth of the generated pulses increases and hence the loss of the pulses in the laser cavity increases, which increases the gain. Therefore, the etalon helps to suppress higher mode pulses with $m \geq 1$. Figure 6 also shows that the dependence of the gain on the detuning $\Delta\Omega$ around the point where the pulse duration is minimal is approximately linear. This result can be obtained from Eq. (6), since when the detuning $\Delta\Omega$ becomes large, the parameter h and hence the parameter P_2 become approximately linear on the detuning difference $|\Delta\Omega - \Delta\Omega_{\min}|$.

We note that at the threshold, the parameter Λ may have an imaginary part. The imaginary part corresponds to a small detuning of the laser frequency. The detuning is equal to $\delta\omega_0 = \mathrm{Im}(\Lambda)/T_R$, where T_R is the round-trip duration. In the example given in Fig. 6, the imaginary part of Λ was significantly smaller than the threshold gain,

$\mathrm{Im}(\Lambda)\approx 4\times 10^{-3}$ and therefore $\delta\omega_0/(2\pi)\approx 1.6$ KHz, assuming that the cavity length $L_c=100$ m. We also note that the term $\mathrm{Im}(\Lambda)$ almost does not affect the parameter $\hat{D}$ in Eq. (26) since $D=0.13\times 10^{-24}$ s^2 while $\mathrm{Im}(\Lambda)/\Omega_g^2=0.13\times 10^{-27}$ s^2.

5. SELECTION OF SUPERMODES BY THE ETALON

Amplitude noise in actively mode-locked lasers can be represented in the frequency domain as a simultaneous lasing of several supermodes [4]. Each supermode consists of a group of coupled cavity modes that are spaced apart by the modulation frequency. The beating between several supermodes that simultaneously lase causes amplitude noise in the laser pulses and even dropout of pulses. For the laser to operate stably, only a single supermode should lase. In the present section, we will show that the etalon suppresses undesired supermodes in the laser as well as locking the central wavelength of the laser pulses. We will also show that the filtering of the intracavity etalon can be approximately three times stronger than the filtering of the same etalon that is connected to the output of the laser.

In Section 3, we assumed that the frequency offset $\delta\omega$ equals 0. This assumption is only accurate when the laser generates a single supermode and when the spectrum of the supermode optimally overlaps the etalon modes and the gain profile of the amplifier. In this section, we will not assume that the frequency offset $\delta\omega$ is equal to zero. We will show that the minimum gain that is required for lasing strongly depends on $\delta\omega$, and therefore, the generation of several supermodes in the laser will be strongly suppressed by the etalon.

When the frequency offset $\delta\omega$ does not equal zero, the steady-state fundamental solution ($m=0$) of the master equation, given in Eq. (19), can be written as

$$\tilde{a}(T,\omega)=A_0\exp\left[-\frac{(\omega+B)^2}{2}\tau^2\right]\exp\left(\frac{T}{T_R}\Lambda\right). \tag{29}$$

Substituting Eq. (29) into Eq. (19) and requiring that the equation is satisfied at each of the powers of the frequency ω, we obtain

$$B=-\frac{\delta\omega}{h/\Omega_M}\frac{\mathrm{Re}(P_2)}{W},$$

$$s\tau^4=W. \tag{30}$$

At threshold we obtain

$$g=\delta-\mathrm{Re}\left[\left(\frac{\delta\omega}{h/\Omega_M}\right)^2\frac{H\,\mathrm{Re}(P_2)}{W}-\sqrt{sW}\right], \tag{31}$$

where $H=W+\mathrm{Re}(P_2)$, while s and W are parameters defined in Eq. (22). Equation (30) determines the pulse duration $2T_0$, the chirp C, and the shift of the laser spectrum B, as a function of the frequency shift $\delta\omega$.

Figure 7 shows the dependence of the threshold gain g_0 on the normalized frequency offset $\delta\omega/\delta\omega_0$ for an etalon with a finesse of $F=200$ and for several values of the frequency detuning between the etalon and the laser modes.

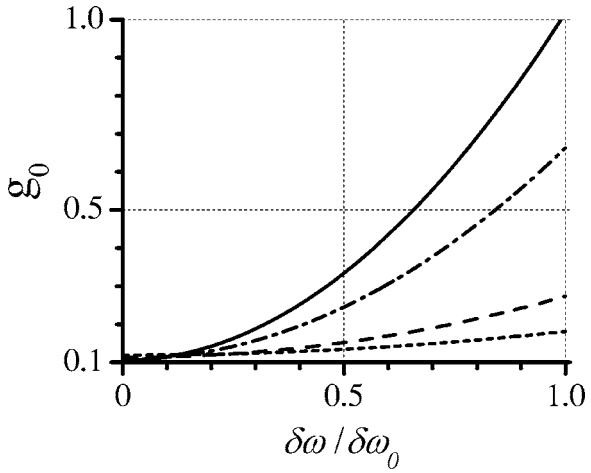

Fig. 7. Dependence of the threshold gain, g_0, on the frequency offset $\delta\omega$, normalized to half of the FWHM of the etalon modes, $\delta\omega_0$, for an etalon with a finesse of $F=200$ with a frequency detuning parameter given by $h/\Omega_M=2\times 10^{-4}$ (dotted curve), 10^{-4} (dashed-dotted curve), 0.5×10^{-4} (dashed curve), 10^{-5} (solid curve).

The frequency offset $\delta\omega$ was normalized to half of the FWHM of the etalon mode, $\delta\omega_0$, where $\delta\omega_0/\Omega_e=2\pi/F$ [12]. Figure 8 shows the threshold gain as a function of the normalized frequency offset $\delta\omega$ for several values of the etalon finesse F. The frequency offset $\delta\omega$ was normalized in this figure to half of the FWHM of an etalon mode with a finesse $F=100$, $\delta\omega_{100}/\Omega_e=2\pi/100$. The frequency detuning parameter was equal to $h/\Omega_M=0.5\times 10^{-4}$. Since the pulse with a minimum duration is obtained when $h\approx 0$, Eq. (6) indicates that h is approximately equal to the detuning $\Delta\Omega-\Delta\Omega_{\min}$.

Several conclusions can be deduced from Figs. 7 and 8. The figures show that the etalon causes a dependence of the threshold gain on the frequency offset $\delta\omega$. Since each supermode has its own frequency offset, the etalon helps to suppress supermode competition. As the threshold gain for a supermode increases, it becomes more difficult for the supermode to lase. Therefore, when the dependence of

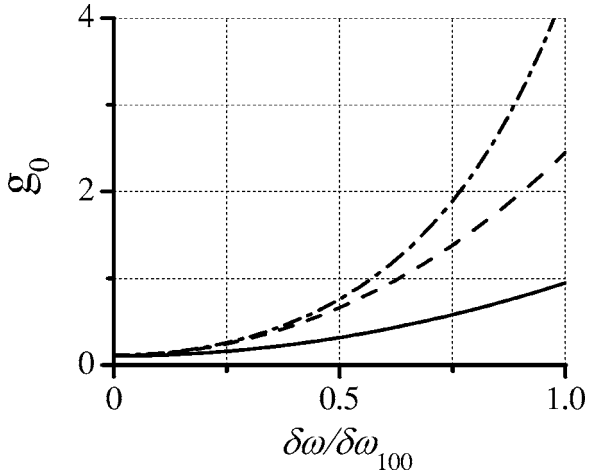

Fig. 8. Dependence of the threshold gain, g_0, on the normalized frequency offset $\delta\omega/\delta\omega_{100}$, where $\delta\omega_{100}$ is half of the FWHM of an etalon with a finesse $F=100$. The values of the etalon finesse are $F=100$ (solid curve), 200 (dashed curve), 400 (dashed-dotted curve). The detuning parameter is given by $h/\Omega_M=0.5\times 10^{-4}$.

the threshold gain on the frequency offset $\delta\omega$ is stronger, the supermode with the lowest gain becomes more stable while the other supermodes are suppressed. Figures 7 and 8 show that the suppression of all but one supermode becomes stronger as the absolute value of the detuning parameter $|h|$ decreases. Therefore, the maximum suppression of the unwanted supermodes is obtained at $h=0$, where a pulse with a minimum duration is generated. Unwanted supermodes are more strongly suppressed as the etalon finesse increases, for a fixed detuning parameter $\Delta\Omega$. However, Fig. 4 shows that the minimum pulse duration also increases as the etalon finesse increases. Therefore, the best combination of strong suppression of all but one supermode with a short pulse duration is obtained for a moderate finesse of the order of several hundreds.

Suppression of unwanted supermodes is obtained even when their frequency offset $\delta\omega$ is significantly smaller than the FWHM of the etalon modes. Therefore, the etalon filtering is significantly stronger than the filtering from the same etalon connected to the output of the laser. This result is obtained since a pulse that propagates in the cavity passes through the etalon on each round trip, and therefore, the effect of the etalon accumulates. For example, when $h=0$ the filtering of etalon at a frequency offset $\delta\omega=\delta\omega_0$ is approximately three times stronger than the filtering of the same etalon connected to the output of the laser. The strong dependence of the threshold laser gain on the frequency detuning $\delta\omega$ also indicates that the etalon helps to lock the central wavelength of the laser to the etalon modes since it promotes the generation of a specific supermode. The supermode that will lase will have the minimum frequency detuning $|\delta\omega|$.

Figure 9 shows the dependence of the carrier frequency offset B on the frequency detuning $\delta\omega$. The carrier frequency offset B minimizes the cavity loss due to the frequency detuning $\delta\omega$. The carrier frequency offset linearly increases as a function of the frequency detuning $\delta\omega$, as shown in Eq. (30). The carrier frequency offset also depends on the parameter h. When the parameter h is equal to zero, the etalon does not filter the laser pulses since $\mathrm{Re}(P_2)=0$, and hence, $B=0$. When the parameter h does not equal to zero the bandwidth and the central frequency of the effective filter created by the etalon depends on the parameter h and the frequency detuning $\delta\omega$. When the parameter h increases ($h>0$), both the bandwidth and the frequency offset of the effective etalon filter decrease. Therefore, the maximum frequency offset is obtained when $h/\Omega_M \approx 7.5\times10^{-5}$.

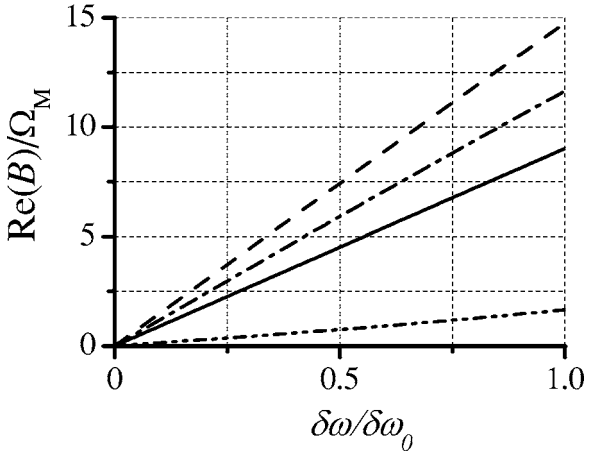

Fig. 9. Dependence of the central frequency offset $\mathrm{Re}(B)$, normalized to the modulation frequency Ω_M, as a function of the frequency offset $\delta\omega$, normalized to half of the FWHM of an etalon mode with a finesse $F=200$, for $h/\Omega_M=2\times10^{-4}$ (solid line) 10^{-4} (dashed line), 5×10^{-5} (dashed–dotted line), and 10^{-5} (dashed–double-dotted line).

6. CONCLUSION

We have theoretically analyzed an actively mode-locked fiber laser with an intracavity etalon by solving the master equation for the laser for the case when nonlinearity can be neglected. We have taken into account the linear dispersion of the material inside the etalon, and we have shown that this dispersion can lead to an increase of the pulse duration by a factor of ~10. The large increase in the pulse duration may be avoided by adding a small frequency detuning between the repetition rate of the laser pulses and the free spectral range of the etalon. The first- and second-order dispersion of the material inside the etalon, as well as the etalon finesse, should be taken into account when calculating the cavity dispersion.

The etalon helps to suppress a simultaneous lasing in several supermodes as well to suppress lasing in higher-order pulse modes of the master equation. The etalon also helps lock the central wavelength of the laser to the etalon comb. Therefore, the use of an intracavity etalon eliminates the need to control the laser cavity as required when the laser is locked to an external etalon [9]. The filtering effect of the etalon can be three times stronger than the effect of the same etalon connected to the output of the laser. By appropriately choosing the cavity dispersion, the etalon finesse, and the dispersion of the material inside the etalon, the minimum pulse duration can be equal to the Kuizenga–Siegman limit of a laser without dispersion. While our work was motivated by the experimental work reported in Refs. [4–7], a detailed comparison of our theory with these experiments was not possible because the cavity dispersion was not exactly reported. We cannot emphasize too strongly that our work shows the importance of both the cavity and the etalon dispersion in determining the pulse duration and hence the importance of carefully determining and optimizing their values in experimental studies.

Nonlinearity in the laser cavity was neglected in this paper. We are currently developing a comprehensive numerical model that will take into account nonlinearity in a laser with an intracavity etalon. Since the intensity inside the etalon is high, it is expected that the etalon will play a significant role in the laser operation. Preliminary results indicate that a small detuning between the etalon and the cavity modes may cause a time shift of the pulses and sometimes even instability in the laser operation.

ACKNOWLEDGMENTS

Work at the Technion was supported in part by a joint grant from the Center for Absorption in Science of the Ministry of Immigrant Absorption of Israel and by the Is-

rael Science Foundation (ISF) of the Israeli Academy of Sciences. Work at the University of Maryland Baltimore County was supported in part by the Naval Research Laboratory.

C. R. Menyuk can be reached via e-mail at menyuk@umbc.edu, and T. F. Carruthers can be reached via e-mail at tcarruth@nsf.gov.

REFERENCES

1. T. R. Clark, T. F. Carruthers, P. J. Matthews, and I. N. Duling III, "Phase noise measurements of ultrafast 10 GHz harmonically modelocked fibre laser," Electron. Lett. **35**, 720–721 (1999).
2. M. E. Grein, H. A. Haus, Y. Chen, and E. P. Ippen, "Quantum-limited timing jitter in actively mode-locked lasers," IEEE J. Quantum Electron. **40**, 1458–1470 (2004).
3. M. Horowitz, C. R. Menyuk, T. F. Carruthers, and I. N. Dulling III, "Theoretical and experimental study modelocked fiber laser for optical communication systems," J. Lightwave Technol. **18**, 1565–1574 (2000).
4. G. T. Harvey and L. F. Mollenauer, "Harmonically mode-locked fiber ring laser with an internal Fabry–Perot stabilizer for soliton transmission," Opt. Lett. **18**, 107–109 (1993).
5. J. E. Malowicki, M. L. Fanto, M. J. Hayduk, and P. J. Delfyett, Jr., "Harmonically mode-locked glass waveguide laser with 21-fs timing jitter," IEEE Photon. Technol. Lett. **17**, 40–42 (2005).
6. S. Gee, F. Quinlan, S. Ozharar, and P. J. Delfyett, Jr., "Simultaneous optical comb frequency stabilization and super-mode noise suppression of harmonically mode-locked semiconductor ring laser using an intracavity etalon," IEEE Photon. Technol. Lett. **17**, 199–201 (2005).
7. J. S. Way, J. Goldhar, and G. L. Burdge, "Active harmonic modelocking of an erbium fiber laser with intracavity Fabry–Perot filters," J. Lightwave Technol. **15**, 1171–1180 (1997).
8. D. J. Kuizenga and A. E. Siegman, "FM and AM mode locking of the homogeneous laser—Part I: theory," IEEE J. Quantum Electron. **QE-6**, 694–708 (1970).
9. R. J. Jones and Jean-Claude Diels, "Stabilization of femtosecond lasers for optical frequency metrology and direct optical to radio frequency," Phys. Rev. Lett. **86**, 3288–3291 (2001).
10. H. A. Haus, "Mode-locking of lasers," IEEE J. Sel. Top. Quantum Electron. **6**, 1173–1184 (2000).
11. Ch. Fabry and A. Perot, "Thérie et applications d'une nouvelle méthode interférentielle," Ann. Chim. Phys. **16**, 115–144 (1899).
12. M. Bass, ed., *Handbook of Optics* (McGraw-Hill, 1995), Vol. 1.
13. S. Choi, M. Yoshida, and M. Nakazawa, "Measurements of longitudinal linewidths of 10 GHz, picosecond mode-locked erbium-doped fiber lasers using a heterodyne detection method," Trans. Inst. Electron. Commun. Eng. Jpn., Part C **J86-C**, 1054–1062 (2003).
14. F. K. Fatemi, J. W. Lou, and T. F. Carruthers, "Frequency comb linewidth of an actively mode-locked fiber laser," Opt. Lett. **29**, 944–946 (2004).
15. G. P. Agrawal, *Nonlinear Fiber Optics* (Academic, 1995), Chap. 1.